

Oxytocin and Vasopressin Receptors in the Pouched Rat

Samanta Arenas^a, Angela R. Freeman^a, Bhupinder Singh^b, Alexander G. Ophir^{*,a}

^aCornell University, Department of Psychology, Ithaca, NY, 14853

^bCornell University, Department of Veterinary Medicine, Ithaca, NY, 14853

Abstract

This is the abstract. It consists of two paragraphs.

Introduction

The neuropeptides, oxytocin (OT) and vasopressin (VP), have receptor distributions in the brain that can modulate a variety of social behaviors such as parental care, affiliation, and aggression, among other behaviors (Caldwell and Albers, 2015). The densities of their associated receptors, oxytocin (OTR) and vasopressin (V1aR and V1bR) receptors, are often species- and sex-dependent.

- What do we know about the distribution and relative densities of receptors (i.e. what can it tell us, what's been done on behavior?)

-How might life history differences play into patterning of central distribution of these receptors?

-What tends to be conserved?

-How does comparative analysis help? (Kelly and Ophir, 2015)

-Why did we do this study? What were we examining?

-We wanted to describe the presence and relative density of OTR and V1aR in pouched rat brains in males and females, to see if there were differences in presence and density between sexes

-We wanted to explore how the patterning of these receptors might differ from other rodents and see if it further supports the ideas found in the recent metaanalysis (Freeman et al., 2020)(see where pouched rats fall in this framework)

Methods

All work with animals was approved under the U.S. Army Medical Research and Materiel Command (USAM-RMC) Animal Care and Use Review Office (ACURO) and the Cornell Institutional Animal Care and Use Committee (IACUC 2014-0043). Tissues were collected from wild-caught animals from Morogoro, Tanzania ($6^{\circ}49'49''S$, $37^{\circ}40'14''E$). Prior to collection, animals were housed individually in standard rabbit enclosures and maintained on

*Corresponding Author

Email addresses: sa658@cornell.edu (Samanta Arenas), arf86@cornell.edu (Angela R. Freeman), bs256@cornell.edu (Bhupinder Singh), ophir@cornell.edu (Alexander G. Ophir)

27 a 12:12 h light:dark light cycle, at 21°C and 45% humidity. Males and females were kept in separate rooms. Animals
28 were fed a standard rodent diet supplemented with dog kibble and fresh fruit and vegetable treats. Chewing bones,
29 a metal ‘stovepipe’ hutch, and dog puzzle toys were given as behavioral enrichment. Newspaper was given for
30 nesting material.

31 Animals were euthanized via CO₂ inhalation and brains were swiftly removed and frozen using liquid nitrogen
32 or powdered dry ice and stored at -80°C prior to sectioning. Ten male and ten female brains were used for this
33 study. Brains were blocked coronally by removing the cerebellum, then split sagittally next to the midline into two
34 hemispheres, and one hemisphere (preferably the left if unblemished) was coronally sectioned at 20µm thick using a
35 Leica cryostat (CM1950, Leica Biosystems, Nussloch, Germany) set at -20°C. Due to the large size of the pouched
36 rat brains, we mounted every 3rd section and kept 6 serial sets. Sections were collected from the olfactory bulbs
37 to the start of the cerebellum, and mounted on Superfrost Plus Microscope sides (Fisher Scientific, Pittsburg, PA
38 USA). Microscope slides were stored at -80°C until the autoradiography procedure.

39 On two of the sets of slides, we used ¹²⁵I radioligands to label oxytocin receptor (ornithine vasopressin analog,
40 ¹²⁵I-OVTA); NEX 254, PerkinElmer; Waltham, MA) or vasopressin 1a receptor (vasopressin (Linear), V-1A antag-
41 onist (Phenylacetyl1, 0-Me-D-Tyr2 [¹²⁵I-Arg6]-); NEX 310, PerkinElmer), as described by Ophir and colleagues
42 (Ophir et al., 2013). Following processing and air-drying, we exposed radiolabeled tissue to film (Kodak Carestream
43 Biomax MS) for 6 days for OTR and 2 days for V1aR to account for differing degrees of decay at the time of use.
44 In each film cassette, we included two ¹²⁵I microscales (American Radiolabeled Chemicals; St Louis, MO), to allow
45 for the conversion of optical density to receptor density. We inferred that receptor density relates to optical density
46 of exposed film to use optical measurements as a proxy for receptor density. We digitized films on a Microtek
47 ArtixScan M1 (Microtek, Santa Fe Springs, CA) and measured optical densities using NIH ImageJ Software. We
48 calculated receptor density by first converting optical density to disintegrations per minute (dpm) adjusted for tissue
49 equivalence (TE; for 1 mg in the rat brain), by fitting curves generated by radiographic standards and extrapolating
50 based on these standard curves for each film.

51 Three sequential sections were measured for density by encircling the regions of interest using NIH ImageJ
52 software. The software program calculated mean optical density values and area for regions of interest (ROI). We
53 measured background labelling by measuring optical density from an area of cortex in the same section for each
54 region of interest. To correctly identify ROI, we Nissl-stained a third set of tissue to use as a reference, in conjunction
55 with anatomical landmarks identified using a Rat brain atlas. The three measurements for each individual’s ROIs
56 and background were averaged separately, and background was subtracted from the ROI to yield receptor density.
57 These final measurements were used for all statistical tests, tables, and figures.

58 OTR density was measured in the olfactory bulb (OB), anterior olfactory nucleus (AON), prefrontal cortex
59 (PFC), piriform cortex (Pir), nucleus accumbens (NAcc), lateral septum (LS), endopiriform (Den), claustrum
60 (VCL), lateral bed nucleus of the stria terminalis (BSTl), medial bed nucleus of the stria terminalis (BSTm),

61 ventral bed nucleus of the stria terminalis (BSTv), ventral pallidum (VPall), medial preoptic area (MPOA), ante-
62 rior hypothalamus (AH), paraventricular thalamus (PVT), suprachiasmatic nucleus (SCN), paraventricular nucleus
63 (PVN), magnocellular hypothalamic nucleus (MCPO), medial habenula (MHb), central amygdala (CeA), medial
64 amygdala (MeA), basolateral amygdala (BLA), ventromedial hypothalamus (VMH), zona incerta (ZIR), lateral
65 hypothalamus (PrFLH), hippocampal CA1, hippocampal CA2, hippocampal CA3, dentate gyrus (DG), premam-
66 milary ventral nucleus (PMV), ventral tegmental area (VTA), periaqueductal gray (PAG), medial geniculate (MG),
67 superior colliculus (SuG), and the ventral CA3. V1aR was measured in the same regions except for the MCPO and
68 the MHb.

69 To calculate ‘relative binding’ on a 4-point scale, we used the following definitions: mean OTR < 35 dpm/mg:
70 absent/-, 35 to 490: present/+, 490 to 945: moderate/++, 945 to 1400: dense/+++; mean V1aR < 100 dpm/mg:
71 absent/-, 100-1367: present/+, 1367 to 2634: moderate/++, 2634 to 3800: dense/+++. To compare receptor
72 densities between sexes, we conducted t-tests for each region. We used a bonferroni correction to adjust for multiple
73 comparisons. Test statistics were considered significant when $p < 0.05$.

74 We used the framework from Freeman et al. (2020) to compare overall binding patterns in the pouched rat to
75 those in other rodents (Freeman et al., 2020). This framework uses overall OTR and V1aR binding patterns to
76 examine similarities among species, genera, and family groups. Briefly, relative binding patterns within a species
77 are converted to a 4-point scale, using wording and data from previously published studies. These data are then
78 used in a principal components analysis, and species are plotted along the PC1 and PC2 components, with vectors
79 in the plot serving as weights of each variable, and the direction indicating loading on PC1 and PC2.

80 We mapped pouched rat relative binding data onto this plot based on this framework and the data presented
81 in this study. In addition to superimposing the pouched rat onto the PCA biplot, we conducted a comparative
82 permutational anova (Adonis function) to examine whether genus or family groups predicted similarities among
83 species’ relative binding patterns using the previously published data and the data from this paper. All analyses
84 were conducted in R 4.0.2, with the vegan package for the ‘adonis’ function, and stats package for t tests and
85 principal components analysis (R Development Core Team, 2016). PCA biplots were made using the ggbiopt
86 function in the ggbiopt package with some aesthetic changes.

87 Results

88 After comparing male and female densities in the measured regions, most regions showed no differences between
89 sexes. The superior colliculus had higher densities of OTR in females compared to males (Table 1, Female mean:
90 199.35, Male mean 51.46, $t_{(13.58)} = 2.79$, $p = 0.01$), however, this was no longer significant after corrections for
91 multiple comparisons (adjusted $\alpha = 0.001$).

Table 1: OTR densities by region and sex

Region	Sex	Density mean \pm SE (dpm/mg)	N
Olfactory Bulb	F	126.27 \pm 39.56	9
Olfactory Bulb	M	142.74 \pm 39.34	9
Accessory Olfactory Nucleus	F	186.38 \pm 40.35	9
Accessory Olfactory Nucleus	M	144.1 \pm 30.98	9
mPFC	F	117.96 \pm 36.91	9
mPFC	M	94.51 \pm 32.08	9
Infralimbic Cortex	F	138.22 \pm 43.25	9
Infralimbic Cortex	M	72.54 \pm 20.32	9
Nac Core	F	46.18 \pm 14.48	9
Nac Core	M	37.34 \pm 12.45	9
Nac Shell	F	81.44 \pm 17.96	9
Nac Shell	M	51.75 \pm 13.37	9
Caudate Putamen	F	30.8 \pm 13.39	9
Caudate Putamen	M	23.93 \pm 8.42	9
Piriform Cortex	F	222.05 \pm 39.71	9
Piriform Cortex	M	192.1 \pm 35.8	9
Lateral Septum I	F	55.24 \pm 12.25	11
Lateral Septum I	M	57.94 \pm 13.57	9
Lateral Septum D	F	48.7 \pm 7.59	11
Lateral Septum D	M	56.22 \pm 12.33	9
Lateral Septum V	F	71.16 \pm 16.63	11
Lateral Septum V	M	103.53 \pm 35.63	9
Endopiriform Cortex	F	147.07 \pm 22.53	10
Endopiriform Cortex	M	111.82 \pm 19.71	9
Clastrum	F	192.58 \pm 47.69	10
Clastrum	M	193.17 \pm 28.09	9
BSTm	F	585.91 \pm 117.64	10
BSTm	M	532.58 \pm 91.23	9
BSTi	F	687.03 \pm 132.48	10
BSTi	M	425.66 \pm 79.05	9
BSTv	F	101.57 \pm 21.35	10

Region	Sex	Density mean \pm SE (dpm/mg)	N
BSTv	M	92.97 \pm 28.24	9
Ventral Pallidum	F	107.32 \pm 15.18	10
Ventral Pallidum	M	78.04 \pm 23.15	9
MPOA	F	95.77 \pm 19.61	10
MPOA	M	88.22 \pm 17.61	9
Anterior Hypothalamus	F	90.27 \pm 24.22	10
Anterior Hypothalamus	M	74.19 \pm 17.25	7
PVT	F	50.91 \pm 16.77	10
PVT	M	64.52 \pm 27.91	7
SCN	F	80.48 \pm 23.44	10
SCN	M	125.57 \pm 45.86	7
PVN	F	14.44 \pm 16.18	9
PVN	M	93.85 \pm 41.77	7
Medial Hypothalamic Nucleus	F	118.68 \pm 37.66	9
Medial Hypothalamic Nucleus	M	122.42 \pm 33.6	7
Medial Habenula	F	545.93 \pm 121.71	10
Medial Habenula	M	648.41 \pm 97.33	9
Central Amygdala	F	695.23 \pm 144.28	9
Central Amygdala	M	734.04 \pm 92.77	9
Medial Amygdala	F	328.84 \pm 51.14	9
Medial Amygdala	M	380.99 \pm 82.29	9
Basolateral Amygdala	F	627.27 \pm 120.17	9
Basolateral Amygdala	M	712.9 \pm 155.24	9
VMH	F	1242.79 \pm 245.41	9
VMH	M	1224.42 \pm 165.26	9
Zona Incerta	F	408.51 \pm 67.31	10
Zona Incerta	M	415.41 \pm 58.07	9
Lateral Hypothalamus	F	176.03 \pm 32.85	10
Lateral Hypothalamus	M	171.5 \pm 41.95	9
CA1	F	121.81 \pm 25.41	11
CA1	M	107.19 \pm 15.49	9
CA2	F	106.13 \pm 11.57	11

Region	Sex	Density mean \pm SE (dpm/mg)	N
CA2	M	127.54 \pm 25.3	9
CA3	F	39.48 \pm 10.47	11
CA3	M	45.77 \pm 10.29	9
Premammillary Nucleus	F	535.99 \pm 110.84	10
Premammillary Nucleus	M	499.3 \pm 106.84	9
VTA	F	523.97 \pm 74.13	9
VTA	M	628.2 \pm 174.1	9
PAG	F	191.21 \pm 35.76	10
PAG	M	106.35 \pm 28.22	7
Superior Colliculus	F	199.35 \pm 46.21	10
Superior Colliculus	M	51.46 \pm 26.08	7

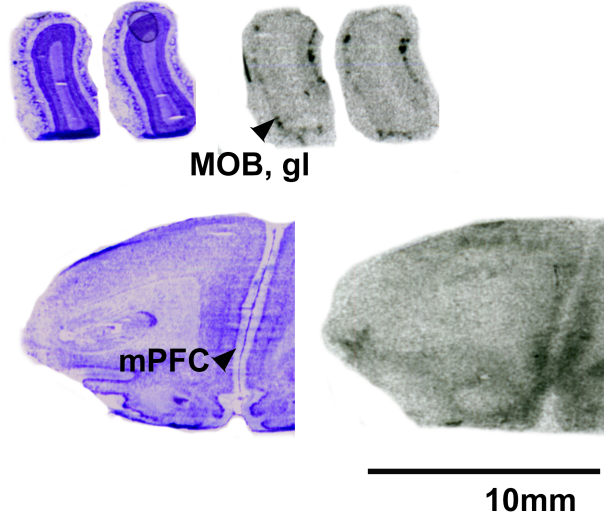


Figure 1: OTR in the forebrain of the pouched rat. Images on left are Nissl stain, associated autoradiograms on right show OTR density. MOB, gl = Main olfactory bulb, glomerular layer, mPFC = medial prefrontal cortex.

92 Pouched rats had very dense OTR binding in the VMH, with moderate binding in the BNST, CeA and VTA.
 93 There was only a low level of binding in the OB and mPFC (Table 2, Figure 1). Extremely low levels of OTR
 94 binding were observed in NAcc, LS, PVN, and thalamus (Figures 2-4).

Table 2: OTR relative densities in select regions

Region	Relative.Binding
Olfactory Bulb	+
Nucleus Accumbens	+
mPFC	+
Ventral Pallidum	-
Lateral Septum	+
BST	++
CeA	++
MeA	+
Hippocampus	+
VMH	+++
VTA	++

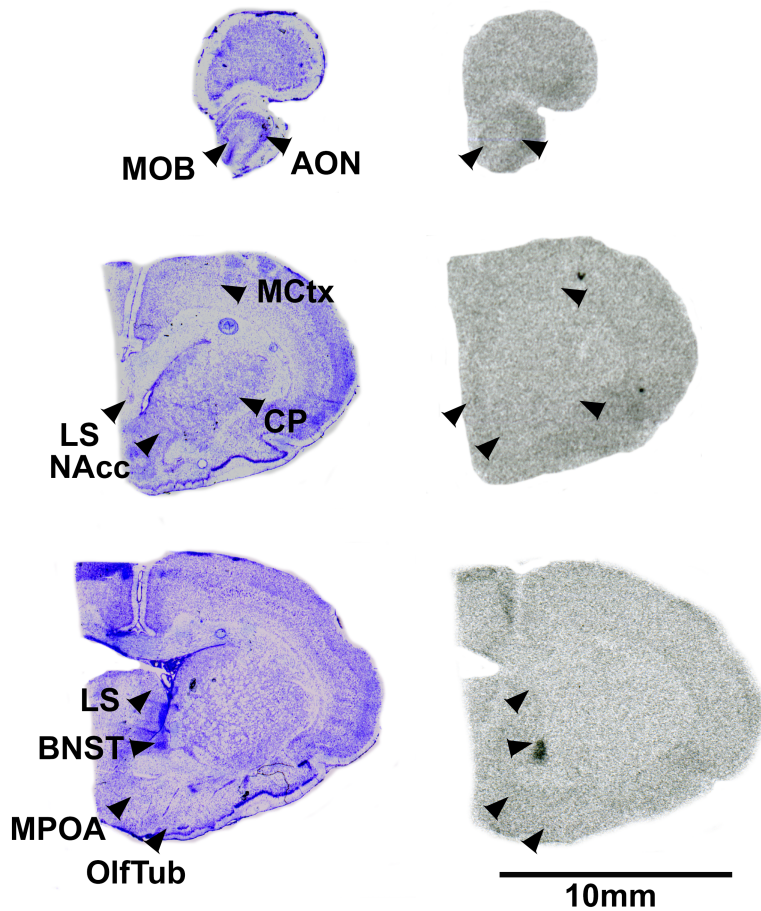


Figure 2: OTR in the forebrain of the pouched rat. Images on left are Nissl stain, associated autoradiograms on right show OTR density. MOB = Main olfactory bulb, AON = accessory olfactory nucleus, LS = lateral septum, CP = caudate putamen, MCtx = motor cortex, NAcc = nucleus accumbens, MPOA = medial preoptic area, OlfTub = olfactory tubercle.

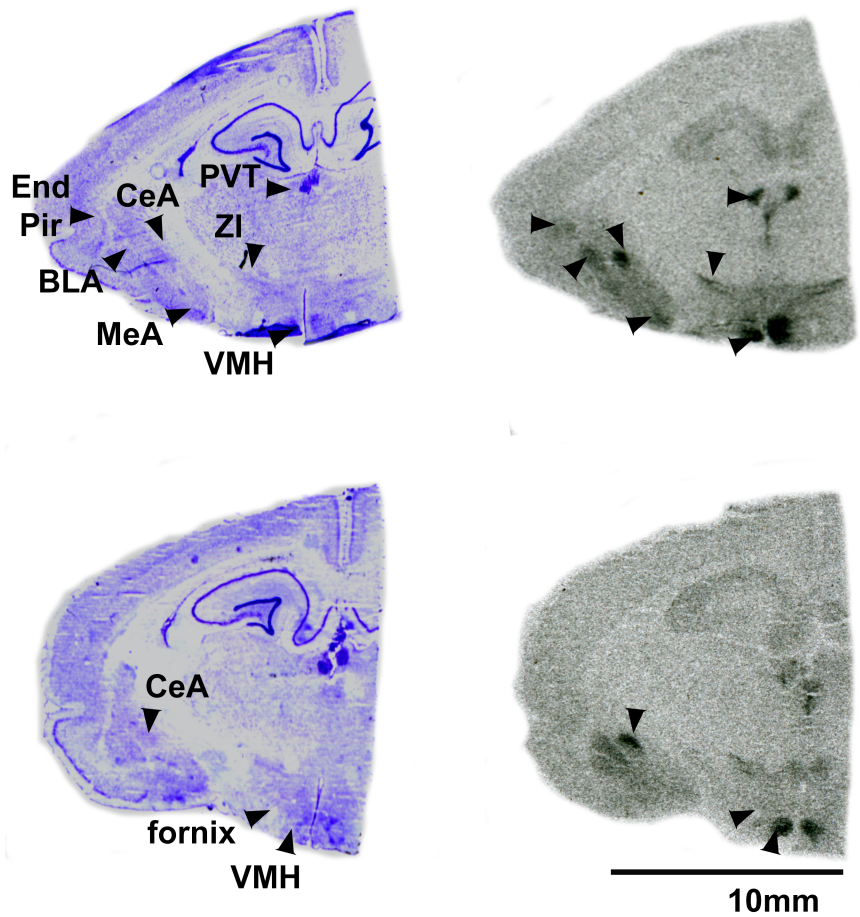


Figure 3: OTR in the forebrain of the pouched rat. Images on left are Nissl stain, associated autoradiograms on right show OTR density. End Pir = Endopiriform Nucleus, BLA = Basolateral Amygdala, MeA = Medial Amygdala, CeA = Central Amygdala, VMH = Ventromedial Hypothalamic Nucleus, ZI = Zona Incerta, PVT = Periventricular Thalamic Nucleus.

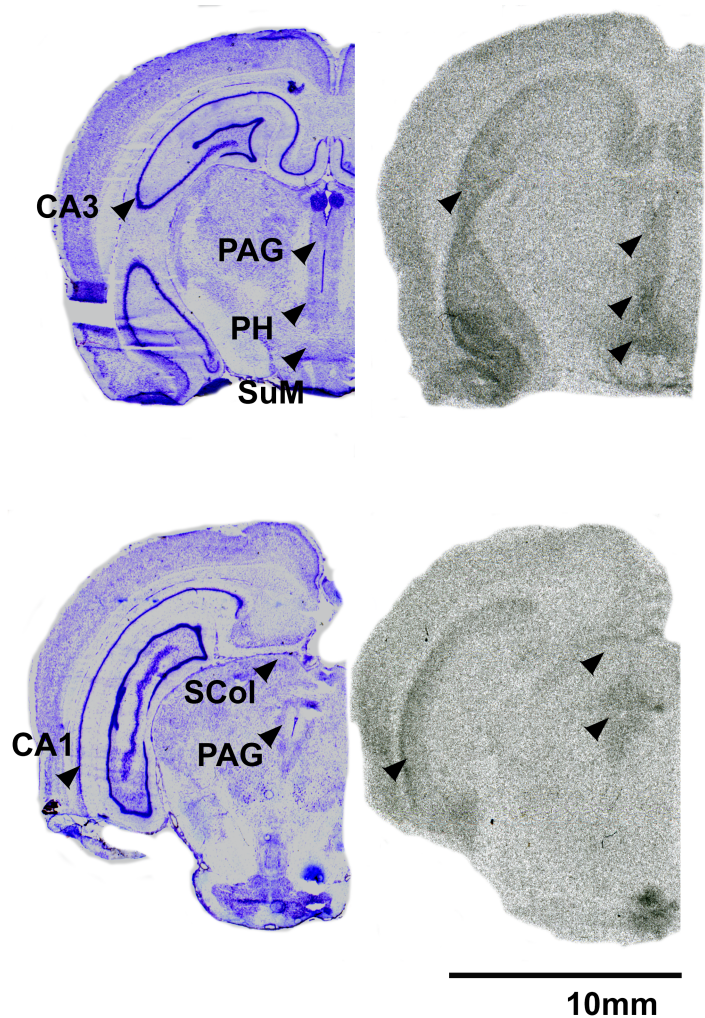


Figure 4: OTR in the forebrain of the pouched rat. Images on left are Nissl stain, associated autoradiograms on right show OTR density. CA3 = CA3 region of the Hippocampus, CA1 = CA1 region of the Hippocampus, PAG = Periacqueductal Grey, PH = Posterior Hypothalamic Nucleus, SCol = Superior Colliculus, SuM = Supramammillary Nucleus

Table 3: V1aR densities by region and sex

Region	Sex	Density mean \pm SE (dpm/mg)	N
Olfactory Bulb	F	1456.47 \pm 244.89	9
Olfactory Bulb	M	1841.49 \pm 278.59	8
Accessory Olfactory Nucleus	F	1287.3 \pm 173.38	9
Accessory Olfactory Nucleus	M	1596.88 \pm 235.76	8
mPFC	F	588.16 \pm 73.53	11
mPFC	M	604.41 \pm 115.62	9
Infralimbic Cortex	F	388.15 \pm 52.78	11
Infralimbic Cortex	M	426.68 \pm 111.74	9
Nac Core	F	1319.1 \pm 113.88	11
Nac Core	M	1748.56 \pm 266.36	8
Nac Shell	F	1389.26 \pm 169.07	11
Nac Shell	M	1687.58 \pm 362.54	9
Caudate Putamen	F	1725.67 \pm 148.69	11
Caudate Putamen	M	2329.94 \pm 322	9
Piriform Cortex	F	604.16 \pm 87.76	11
Piriform Cortex	M	649.05 \pm 144.85	9
Lateral Septum I	F	3602.8 \pm 355.47	11
Lateral Septum I	M	2885 \pm 369.04	9
Lateral Septum D	F	3451.24 \pm 276.7	11
Lateral Septum D	M	3613.44 \pm 207.77	9
Lateral Septrum V	F	2395.85 \pm 311.31	11
Lateral Septrum V	M	2351.65 \pm 325.22	9
Endopiriform Cortex	F	296.6 \pm 58.56	11
Endopiriform Cortex	M	260.42 \pm 57.86	9
Clastrum	F	446.08 \pm 74.68	11
Clastrum	M	334.95 \pm 58.2	9
BSTm	F	1552.05 \pm 161.04	11
BSTm	M	1452.1 \pm 229.77	9
BSTi	F	1297.66 \pm 80.59	11
BSTi	M	1056.38 \pm 188.24	9
BSTv	F	885.07 \pm 108.44	11

Region	Sex	Density mean \pm SE (dpm/mg)	N
BSTv	M	835.57 \pm 116.42	9
Ventral Pallidum	F	616.94 \pm 104.42	11
Ventral Pallidum	M	470.4 \pm 142.24	9
MPOA	F	626.46 \pm 84.5	11
MPOA	M	522.26 \pm 75.01	9
Anterior Hypothalamus	F	364.98 \pm 97.49	9
Anterior Hypothalamus	M	601.09 \pm 288.18	8
PVT	F	63.75 \pm 58.22	9
PVT	M	245.11 \pm 131.63	8
SCN	F	207.91 \pm 109.3	9
SCN	M	85.55 \pm 71.97	8
PVN	F	514.58 \pm 146.84	8
PVN	M	520.91 \pm 161.33	7
Central Amygdala	F	1710.61 \pm 186.92	10
Central Amygdala	M	1439.79 \pm 188.75	9
Medial Amygdala	F	841.82 \pm 76.12	10
Medial Amygdala	M	928.64 \pm 160.08	9
Basolateral Amygdala	F	120.35 \pm 66.19	10
Basolateral Amygdala	M	139.62 \pm 74.36	9
VMH	F	390.55 \pm 130.5	10
VMH	M	576.42 \pm 141.68	9
Zona Incerta	F	705.31 \pm 78.81	10
Zona Incerta	M	738.07 \pm 94.39	9
Lateral Hypothalamus	F	745.93 \pm 91.88	10
Lateral Hypothalamus	M	915.03 \pm 143.4	9
CA2	F	119.25 \pm 56.35	11
CA2	M	63.4 \pm 81.27	9
Dentate Gyrus	F	281.61 \pm 107.99	11
Dentate Gyrus	M	347.83 \pm 172.25	9
Premammillary Nucleus	F	1458.58 \pm 333.09	11
Premammillary Nucleus	M	2206.81 \pm 616.26	9
VTA	F	1132.57 \pm 186.43	11

Region	Sex	Density mean \pm SE (dpm/mg)	N
VTA	M	1278.42 \pm 203.04	9
PAG	F	734.99 \pm 97.71	11
PAG	M	947.68 \pm 293.67	7
Medial Geniculate	F	93.87 \pm 50.87	11
Medial Geniculate	M	147.82 \pm 117.32	7
Superior Colliculus	F	819.1 \pm 146.2	11
Superior Colliculus	M	744.4 \pm 229.16	7
Ventral CA3	F	67.1 \pm 78.53	5
Ventral CA3	M	119.62 \pm 148.52	2

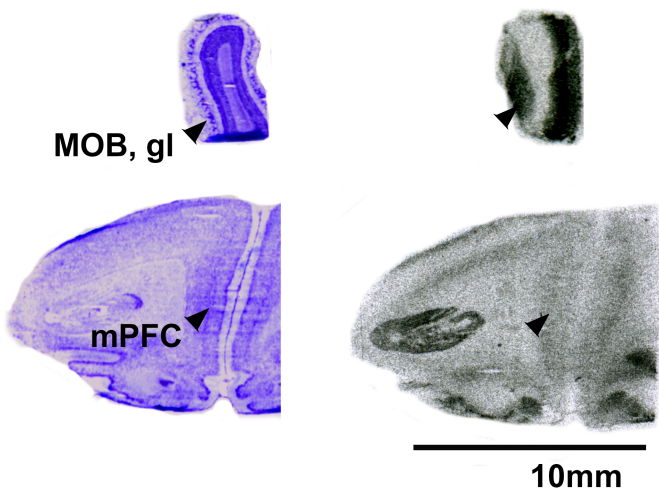


Figure 5: V1aR in the forebrain of the pouched rat. Images on left are Nissl stain, associated autoradiograms on right show V1aR density. MOB, gl = Main olfactory bulb, glomerular layer, mPFC = medial prefrontal cortex.

95 After comparing male and female densities of V1aR in the measured regions, we detected no significant differences
 96 between sexes (Table 3).

97 Pouched rats had relatively very dense V1aR binding in the LS (Figure 6), and moderately dense levels of V1aR
 98 binding in the Olfactory Bulbs, BST, NAcc, Amygdalar and Hypothalamic Nuclei (Figures 5-10). Binding in the
 99 Hippocampus was generally absent except for some moderate V1aR binding in the most ventral regions (Figure
 100 10).

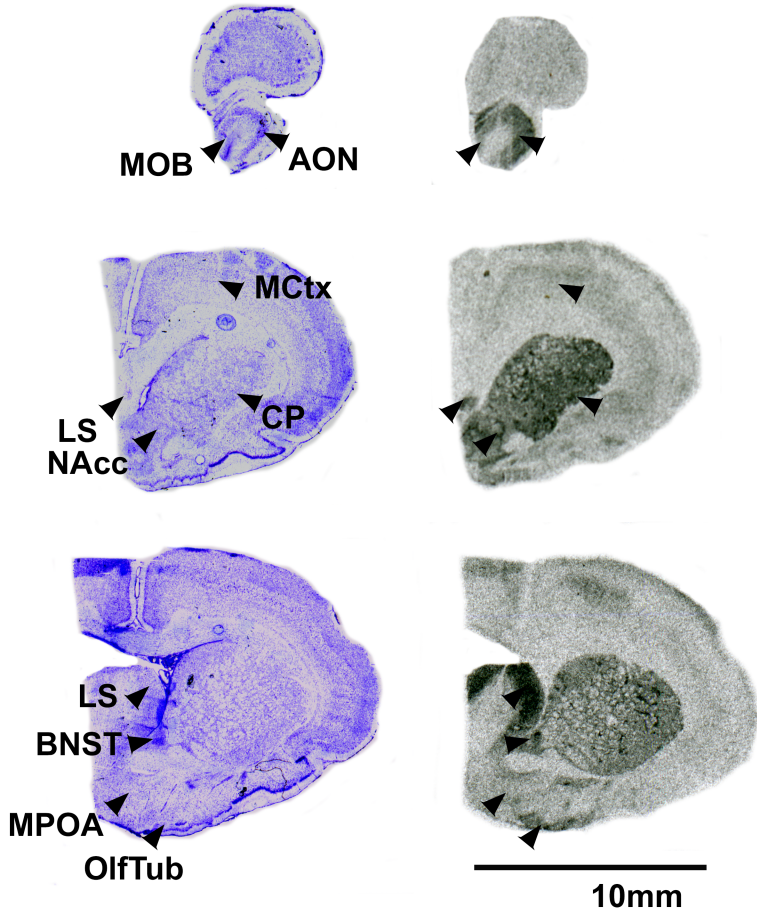


Figure 6: V1aR in the forebrain of the pouched rat. Images on left are Nissl stain, associated autoradiograms on right show V1aR density. MOB = Main olfactory bulb, AON = Accessory Olfactory Nucleus, LS = Lateral Septum, NAcc = Nucleus Accumbens, CP = Caudate Putamen, BNST = Bed Nucleus of the Stria Terminalis, MCtx = Motor Cortex, MPOA = Medial Preoptic Area, OlfTub = Olfactory Tuber.

Table 4: V1aR relative densities in select regions

Region	Relative.Binding
Olfactory Bulb	++
Nucleus Accumbens	++
mPFC	+
Ventral Pallidum	+
Lateral Septum	+++
BST	++
CeA	++
MeA	+
PVN	+

Region	Relative.Binding
Hippocampus	-
Dentate Gyrus	+
Premammillary Nucleus	++
VMH	+
VTA	+

Table 5: V1aR Maximized species Permutational Manova by family

	Df	SS	MS	F	R ²	p
Family pg	5	0.4106237	0.0821247	1.464944	0.3603847	0.1188811
Residuals	13	0.7287799	0.0560600	NA	0.6396153	NA
Total	18	1.1394035	NA	NA	1.0000000	NA

Table 6: V1aR Maximized species Permutational Manova by genus

	Df	SS	MS	F	R ²	p
my genus	11	0.9294802	0.0844982	2.817636	0.8157604	0.007992
Residuals	7	0.2099233	0.0299890	NA	0.1842396	NA
Total	18	1.1394035	NA	NA	1.0000000	NA

Comparing the overall patterns of binding of OTR to other rodents, the pouched rat was most similar in OTR binding to *Microtus* voles due to low binding in the hippocampus, but relatively high binding in the VMH (Figure 11). In these PCA biplots, the relative location of a species represents its pattern of binding in the regions identified at the end of the vectors. Therefore, species with similar receptor binding patterns will be positioned close together in the plot. The direction of these brain region vectors (i.e. arrows) indicates relative loading on PC1 and PC2, and the length of the vector indicates the weight associated with the two principal components. Therefore, a species placed near the end of a vector typically indicates relatively dense binding in that region compared to other regions in the plot.

When the number of species included in the analysis was maximized, the pouched rat was placed relatively centrally in the plot, and clustered with a number of other rodents, suggesting that the overall patterns of OTR binding in the pouched rat brain in these regions were very similar to a most other studied rodents (Figure 12).

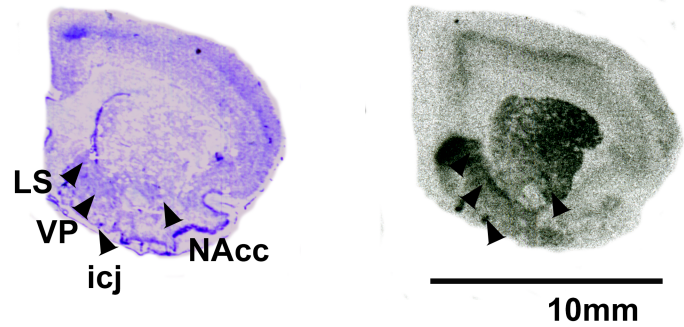


Figure 7: V1aR in the forebrain of the pouched rat. Image on left is Nissl stain, associated autoradiogram on right shows V1aR density. LS = Lateral Septum, NAcc = Nucleus Accumbens, VP = Ventral Pallidum, icj = Islands of Calleja.

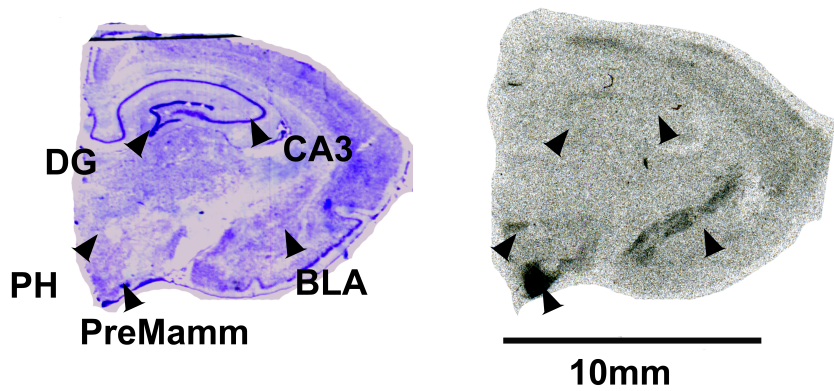


Figure 8: V1aR in the forebrain of the pouched rat. Image on left are Nissl stain, associated autoradiogram on right shows V1aR density. DG = Dentate Gyrus, CA3 = CA3 Region of the Hippocampus, BLA = Basolateral Amygdala, PH = Posterior Hypothalamus, PreMamm = Premammillary Nucleus.

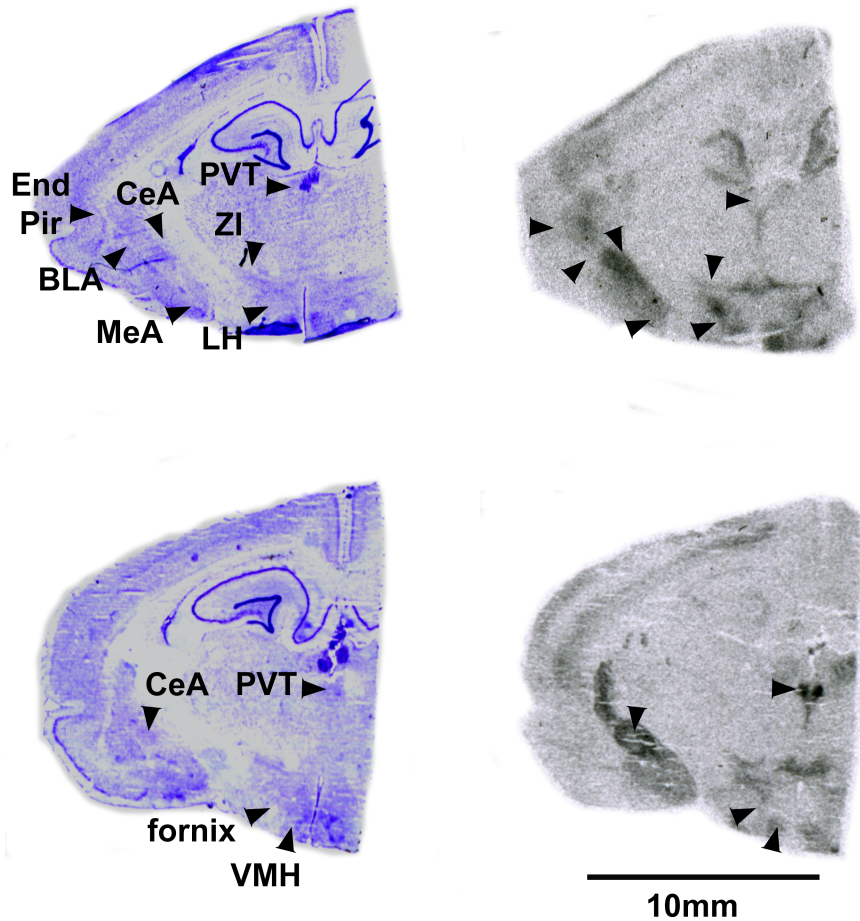


Figure 9: V1aR in the forebrain of the pouched rat. Image on left are Nissl stain, associated autoradiogram on right shows V1aR density. End Pir = Endopiriform Nucleus, BLA = Basolateral Amygdala, MeA = Medial Amygdala, CeA = Central Amygdala, VMH = Ventromedial Hypothalamic Nucleus, ZI = Zona Incerta, PVT = Periventricular Thalamic Nucleus, LH = Lateral Hypothalamus.

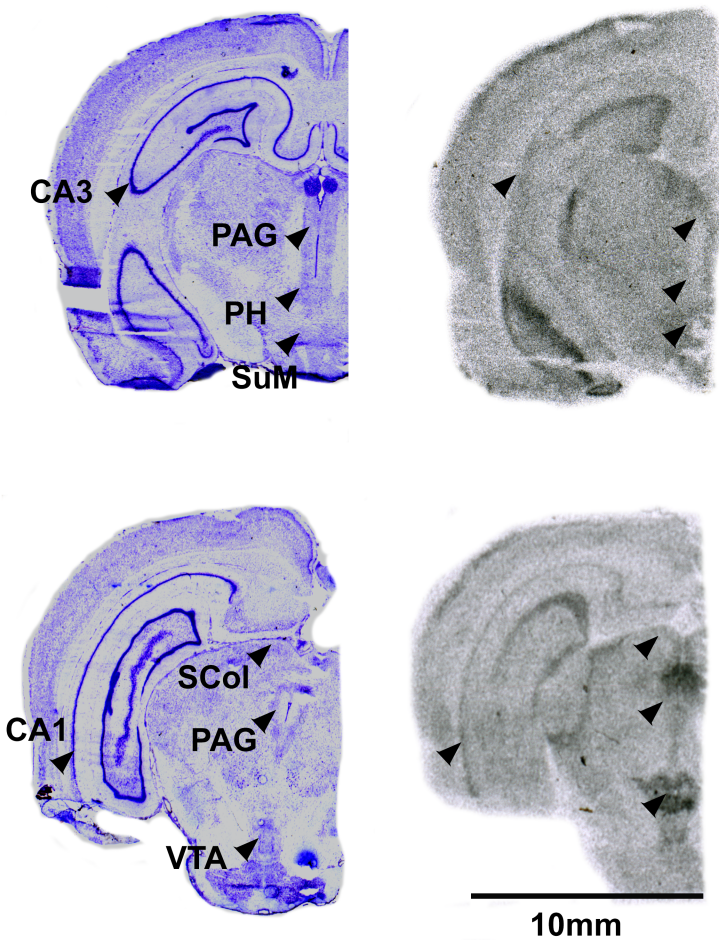


Figure 10: V1aR in the forebrain of the pouched rat. Image on left are Nissl stain, associated autoradiogram on right shows V1aR density. CA3 = CA3 region of the Hippocampus, CA1 = CA1 region of the Hippocampus, PAG = Periacqueductal Grey, PH = Posterior Hypothalamic Nucleus, SCol = Superior Colliculus, SuM = Supramammillary Nucleus, VTA = Ventral Tegmental Area.

a	Cavia	a	Heterocephalus	a	Mus	a	Rattus
a	Cricetomys	a	Meriones	a	Octodon	a	Scotinomys
a	Ctenomys	a	Microtus	a	Otomys	a	Urocitellus

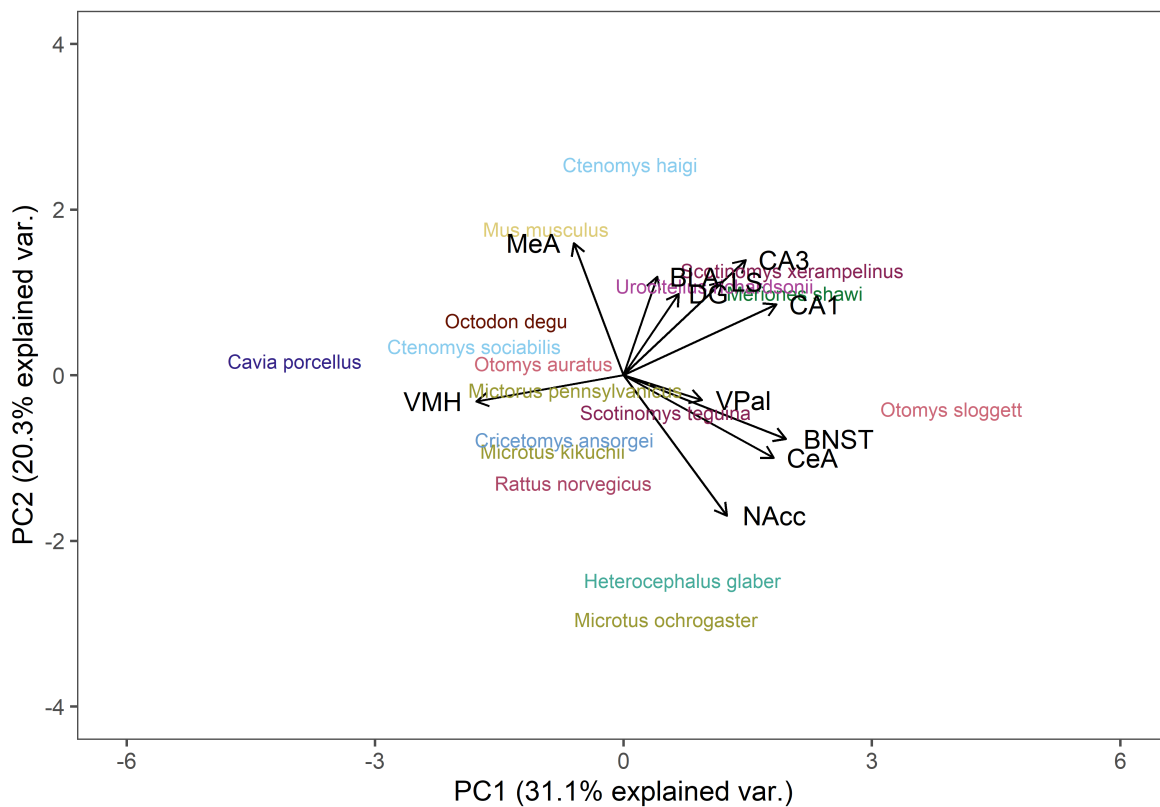


Figure 11: a PCA, OTR with regions maximized

112 The multivariate comparison of V1aR binding, with the number of species included maximized, showed that
 113 the pouched rat was placed relatively close to the hamsters (*Phodopus sungorus*, *Meriones shawi* and *Meriones*
 114 *unguiculatus*). However, when the number of regions included was increased, the pouched rat became more distant
 115 from these hamsters, indicating that binding patterns in these newly included regions (the Hippocampal regions and
 116 Basolateral amygdala) were different between hamsters and the pouched rat and resulted in additional variance. In
 117 this analysis, with the number of regions included maximized, the pouched rat is placed between the peromyscus
 118 mice and the microtus voles in the plot.

a	Cavia	a	Georychus	a	Mesocricetus	a	Octodon	a	Rattus
a	Cricetomys	a	Heterocephalus	a	Microtus	a	Otomys	a	Scotinomys
a	Ctenomys	a	Meriones	a	Mus	a	Peromyscus	a	Urocitellus

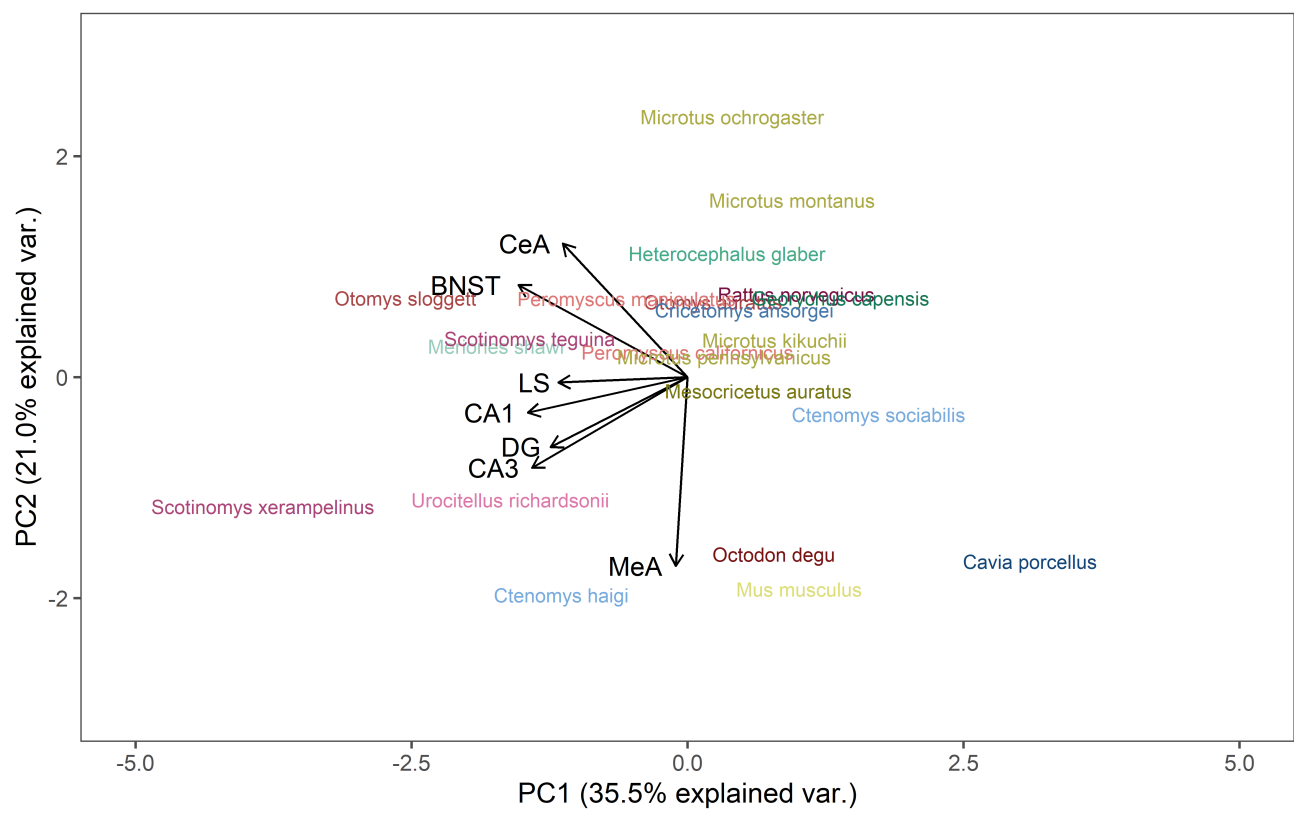


Figure 12: a PCA, OTR with species maximized

a	Cricetomys	a	Meriones	a	Mus	a	Rattus
a	Ctenomys	a	Mesocricetus	a	Peromyscus	a	Scotinomys
a	Jaculus	a	Microtus	a	Phodopus	a	Urocitellus

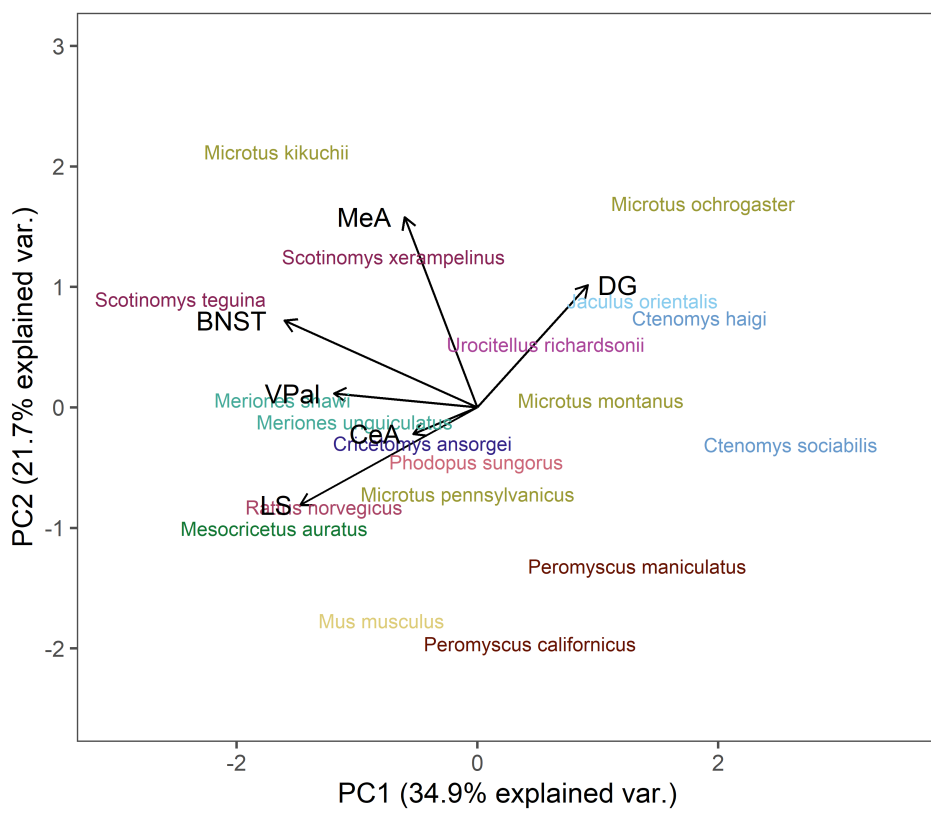


Figure 13: a PCA, V1aR with species maximized

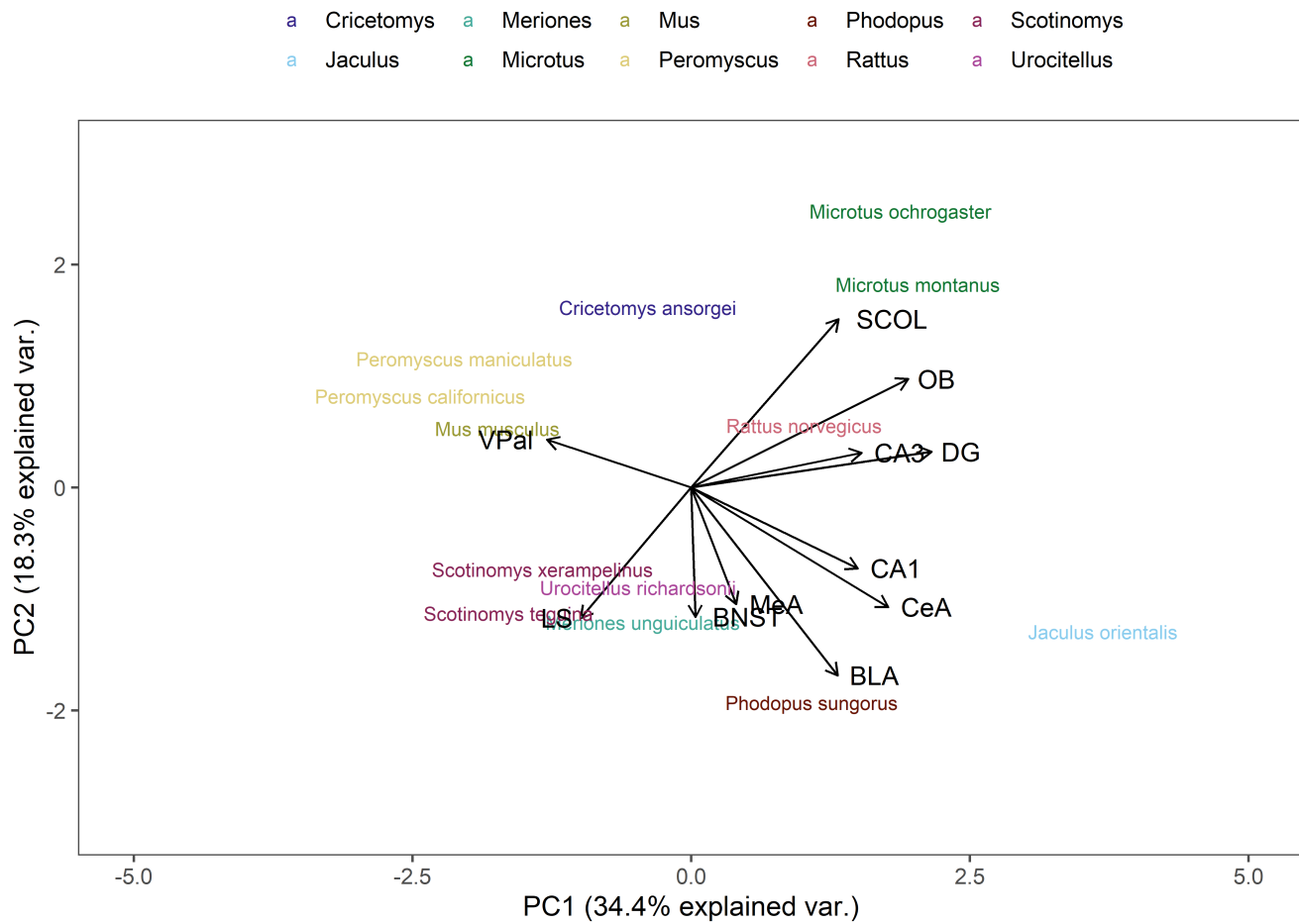


Figure 14: a PCA, V1aR with regions maximized

119 **Discussion**

- 120 -We found OTR in ... V1aR in....
- 121 -Sex differences in densities/presence and absence
- 122 -We found that overall patterns were similar to....
- 123 -Caveats
- 124 -Unknown age
- 125 -Unknown reproductive status
- 126 -Different experiences possible
- 127 -What this means, similarities to other species
- 128 -Relevance for behavior or life history
- 129 What still needs to be known?

130 **References**

- 131 Caldwell, H.K., Albers, H.E., 2015. Oxytocin, vasopressin, and the motivational forces that drive social behav-
132 iors, in: Behavioral Neuroscience of Motivation. Springer, pp. 51–103. doi:10.1007/7854
- 133 Freeman, A.R., Aulino, E.A., Caldwell, H.K., Ophir, A.G., 2020. Comparison of the distribution of oxytocin
134 and vasopressin 1a receptors in rodents reveals conserved and derived patterns of nonapeptide evolution. Journal
135 of Neuroendocrinology 32, e12828. doi:10.1111/jne.12828
- 136 Kelly, A.M., Ophir, A.G., 2015. Compared to what: What can we say about nonapeptide function and social
137 behavior without a frame of reference? Curr Opin Behav Sci 6, 97–103. doi:10.1016/j.cobeha.2015.10.010
- 138 Ophir, A.G., Sorochman, G., Evans, B.L., Prounis, G.S., 2013. Stability and dynamics of forebrain V1aR and
139 OTR during pregnancy in prairie voles. Journal of neuroendocrinology 25, 719–728. doi:10.1111/jne.12049
- 140 R Development Core Team, 2016. R: A language and environment for statistical computing. R Foundation for
141 Statistical Computing, Vienna, Austria. URL <http://www.R-project.org/>, R Foundation for Statistical Computing,
142 Vienna, Austria. doi:10.1007/978-3-540-74686-7